IJCRT.ORG ISSN : 2320-2882

INTERNATIONAL JOURNAL OF CREATIVE RESEARCH THOUGHTS (IJCRT)

An International Open Access, Peer-reviewed, Refereed Journal

GENERATION OF VOLTAGE FROM A PIEZOLAMINATED PARABOLIC TAPERED CANTILEVER BEAM USING FINITE ELEMENT METHOD

[1] Alok Ranjan Biswal [2] Mahabir Biswal [3] Manoj Kumar Mallick [4]Lingaraj Nath

[1] Associate professor, [2] M Tech Research Scholar, [3] M Tech Research Scholar [4] M Tech Research Scholar

[1] Mechanical Engineering,

[1] DRIEMS Autonomous, Odisha, India

Abstract: Structural analysis plays a crucial role in the recent era for nonprismatic beams with different cross section, material properties and many more. Due to high moment resistance and aesthetic nature these beams are widely used. But during service condition these beams undergoes vibration where most of the energies is getting lost. If this energy can be saved in electrical form, then it could be used in different fields further. Taking into consideration of the coupling of electro mechanical system the present article deals with the finite element (FE) based modelling and analysis of a parabolic tapered piezolaminated cantilever beam for voltage generation. The Euler-Bernoulli beam theory has been used in this approach. The governing equation of motion for the proposed beam has been derived by the Hamilton's principle. In order to solve the governing equation two noded beam element with two degrees of freedom (DOF) per node has been considered. In this work the effect of structural damping has also been incorporated in the finite element model. The effects of taper (both width and height direction) on output voltage have been discussed.

Keywords: **Finite element method, Euler-Bernoulli beam, Piezoelectricity**

I. INTRODUCTION

Due to the flexible properties, piezoelectric structural materials can function as both sensors and actuators for monitoring and controlling the response of a structure. In sensor applications, the strains in the piezoelectric material can be determined by measuring the induced electric potential. Piezoelectric materials have been widely used in many applications. The piezoelectric unimorph and bimorph, which can produce flexural deformation significantly larger than the length or thickness deformation of the individual piezoelectric layers, have been used as electro acoustic transducers, medical devices, micro robot, and atomic force microscope cantilevers due to the characteristics of miniaturization, high positioning accuracy, sensitive response, and large displacement [1] In actuator applications, distributed forces can be affected by subjecting the piezoelectric material to an appropriate electric potential. The phenomenon of piezoelectricity is useful for controlling the static and dynamic response of various smart structures involving the process of transfer of energy between the mechanical domain to electric domain and vice versa. Among the possibilities for voltage generators, piezoelectric materials have been generally more predominant because of their strong ability to convert ambient mechanical energy into electrical energy[2]. Lead Zirconate Titanate (PZT) is the most used piezoelectric material because of its high electromechanical coupling characteristics in single crystals [3]. The use of piezoelectric elements attached to vibrating beam was studied to convert mechanical vibration energy for possible application in powering wireless sensor nodes [4] In. that work it has been found that when a piezoelectric energy harvester device was made to operate at frequency matching the vibrating frequency that is at resonance, the output electrical power generated was maximized. Meanwhile, an analytical model of a beam was developed with attached PZT elements to provide an accurate estimate of the power generated by the piezoelectric effect. The analysis of piezoelectric composite structures such as piezoelectric laminated plates and beams requires efficient and accurate electromechanical modelling of both the mechanical and electric responses such as mechanical displacements and electric potentials. The accurate response of these structures can be obtained by solving the three dimensional (3D) coupled field equations with exact satisfaction of the mechanical and electric boundary conditions and inter laminar continuity conditions [5]. A detailed bibliographical review of the finite element methods applied to the analysis and simulation of smart piezoelectric materials and structures can be found in [6].

Non-prismatic beams whose cross-section profile changes gradually along their length are of great importance in different fields of engineering. The advantages of using these beams due to their ability in meeting the architectural and

aesthetical needs and optimizing the weight and strength of the structure. This particular advantage of non-prismatic members plays a very important role in construction and performance of aerospace structures. The study of cantilevered vibration energy harvesters has been focused on different aspects with the overall goal being to optimize the performance of existing devices. A model of rectangular cantilevered vibration energy harvester was developed with different lengths and widths in order to explore how the beam dimensions affected the matching resistance and power output [7] Results in their study have shown that with the same length, the wider rectangular cantilevered vibration energy harvester can generate more than twice the power output. A commercial finite element analysis (FEA) code ANSYS to explore the influence of dimensions on the current and power output of rectangular cantilevered vibration energy harvester, including the length, width and thickness of vibration energy harvester as well as tip masses. The study suggested that a wider but shorter beam was preferred since it generated larger current and power output [8]. However, the resonance frequencies in their models were varied and the base acceleration inputs were incorrectly normalized. The design of rectangular cantilevered vibration energy harvester have optimised by changing the geometrical parameters and including large tip masses in order to achieve a fixed resonance frequency [9]. The exact solution of differential equation in the linear case of free bending vibrations of nonuniform beam with rectangular cross-section using the factorization method. This beam with constant width and parabolic thickness is a good approximation of the gear tooth profile. The case of the beam with a sharp end is considered [10] .Free vibration of nonuniform rotating beam which has circular cross section and the differential equation in term of hyper geometric function has been studied. The transverse vibration of beam in two cases of cross section where the first case of circular cross section which had both ends sharp and the second case was rectangular cross section for beam of one end sharp have been discussed [11] The mathematical model and numerical method for free vibration of tapered piles embedded in two-parameter elastic foundations has been studied [12]. Euler-Bernoulli beam theory has been considered for the analysis. The results prove that the proposed method is quite easy to implement, accurate and highly efficient for free vibration analysis of tapered beam-columns embedded in Winkler- Pasternak elastic foundations.

The present article exclusively focused on generation of voltage from the piezolaminated tapered cantilever beam by using finite element analysis. The governing equation of motion has been derived by using Hamilton's principle. In order to solve the governing equation two noded beam element with two degrees of freedom (DOF) per node has been considered. The effect of structural damping has also been incorporated in the finite element model. The effects of taper (both the width and height direction) on output voltage from non-prismatic beam is discussed and compared with the prismatic beam.

II. MATHEMATICAL FORMULATION

The mathematical formulations of the present analysis involve the modelling of cross section of the beam, finite element modelling and analysis of piezolaminated beam which are described in the following sections.

2.1. MODELLING OF CROSS SECTION OF THE BEAM

In order for modelling the cross section of the beam the proposed shape function profile has been considered as

$$A(x) = A_0\left(1 - r_b \frac{x}{L}\right)^2\left(1 - r_h \frac{x}{L}\right)^2 \quad (1)$$

Where L is the length of the beam and A_0 is the cross section area of the beam near the clamped end. The breadth and height taper ratio are represented as r_b and r_h respectively and could vary in the range of 0 to 1.

2.2. FINITE ELEMENT MODELLING OF PIEZOLAMINATED BEAM

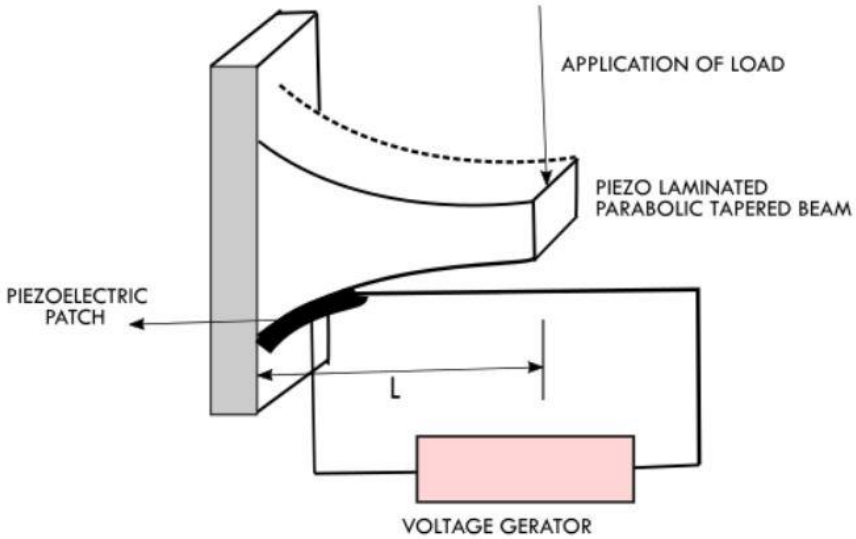

Figure 1 Piezolaminated parabolic tapered beam with voltage generator

Figure 1 shows a cantilever beam of length 'L', subjected to a point load acting at its free end. A piezoelectric strip of length 'L_p' is attached in the cantilever beam near the fixed end. The mechanical and electrical behaviour of a piezoelectric material can be modelled by two linearized constitutive equations. These equations contain two mechanical and two electrical variables. The direct effect and the converse effect may be modelled by the following matrix equations [13]

$$\{T\}=[c]\{S\}-[e]^T\{E\} \quad (2)$$
$$\{D\}=[e]\{S\}+[\varepsilon]\{E\}$$

Where$\{T\},\{S\}$ are longitudinal stress and strain, $[c]$ is the compliance matrix, $\{E\}$ is the effective electric field, $\{D\}$ is the electric displacement, $[e]$ is the piezoelectric coupling coefficient and $[\varepsilon]$ is the permittivity. The dynamic equations of the system for voltage generation are derived using Hamilton's principle.

$$\partial\Psi=\int_{t_1}^{t_2}\left[\partial\left(KE-PE+W_p\right)\right]dt=0 \quad (3)$$

Where '∂' is the variation, t_1 and t_2 are the starting and finish time, *KE* is the total kinetic energy, *PE* is the total potential energy and *Wp* is the total work done by the external mechanical and electrical force. The sum of (*KE*−*PE*+*Wp*) is called the Lagrangian *L*a.

$$KE=\frac{1}{2}\int_{V_b}S^T T dV_b+\frac{1}{2}\int_{V_p}S^T T dV_p-\frac{1}{2}\int_{V_p}E^T D dV_p \quad (4)$$

$$PE=\int_{V_b}\rho_b\dot{w}^T\dot{w}dV_b+\int_{V_p}\rho_b\dot{w}^T\dot{w}dV_p \quad (5)$$

$$W_p=\sum_{i=1}^{n_f}\partial w(x_i).Q_i(x_i) \quad (6)$$

V is the volume, *w* is the displacement, *x* is the position along the beam, *v* is the applied voltage, *q* is the charge, ρ is the density and the subscripts *b* and *p*, represent the beam and the piezoelectric material respectively. Now putting Eqs. (2), (4), (5) and (6) in Eq. (3) we get

$$\partial\psi=\int_{t_1}^{t_2}\left[\begin{array}{l}\int_{V_b}\rho_b\delta\dot{w}^T\dot{w}dV_b+\int_{V_p}\rho_p\delta\dot{w}^T\dot{w}dV_p-\int_{V_b}\delta S^T c^S S dV_b-\int_{V_p}\delta S^T c^S S dV_p+\int_{V_p}\delta S^T e^T E dV_p\\ +\int_{V_p}\delta E^T e S dV_p+\int_{V_p}\delta E^T\varepsilon^S E dV_p+\sum_{i=1}^{n_f}\partial w(x_i)Q(x_i)\end{array}\right] \quad (7)$$

This equation can now be used to solve for the equations of motion of any mechanical system containing piezoelectric elements. Considering the finite element procedure of the proposed modelled beam, the beam element is shown in Fig.2. with all degrees of freedom at each nodes.

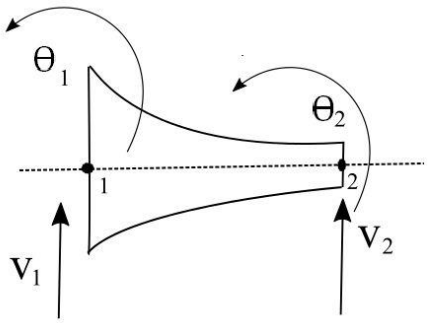

Figure 2 Nodal degrees of freedom of the proposed parabolic tapered beam element

The displacement field in terms of shape function can be represented as

$$w(x,t)=[N_w]\{q\} \quad (8)$$
$$w'(x,t)=[N_\theta]\{q\}$$

Where $[N_w]$ and $[N_\theta]$ are the shape functions for displacement and rotation and $\{q\}$ is the nodal displacements. The element has been assumed with one electrical degree of freedom at the top of piezoelectric patch. The voltage has been assumed to be constant over an element and vary linearly through the thickness of piezoelectric patch. For a thin piezoelectric patch, the component of the electric field in the thickness direction is dominant. Therefore the electric field can be accurately approximated with a non-zero component only in the thickness direction.

$$-E=[B_V]\{v\}=\left[\frac{1}{t_p}\right]\{v\} \quad (9)$$

Using the above equations the variational indicator has been found to include terms that represent physical parameters. By doing this the equations describing the system become more recognizable when compared to those of a typical system and help give physical meaning to the parameters in the equations of motion. By solving the governing equation the mass matrix for the system for both beam element and piezo element can be derived as

$$[m_b] = \int_0^{L_b} [N_w]^T \rho_b A_b [N_w] dx$$
$$\text{and } [m_p] = \int_0^{L_p} [N_w]^T \rho_p A_p [N_w] dx \quad (10)$$

Similarly the stiffness matrix for the beam and the piezo element can be derived as

$$[k_b] = \int_0^{L_b} \left[\frac{\partial [N_w]}{\partial x}\right]^T E_b I_b \left[\frac{\partial [N_w]}{\partial x}\right] dx$$
$$\text{and } [k_p] = \int_0^{L_p} \left[\frac{\partial [N_w]}{\partial x}\right]^T E_p I_p \left[\frac{\partial [N_w]}{\partial x}\right] dx \quad (11)$$

From the governing equation the electromechanical coupling matrix, k_{pb}, and the capacitance matrix, k_{pp}, have been found which can be represented as

$$[k_{pb}] = -\int_{V_p} z \left[\frac{\partial [N_\theta]}{\partial x}\right]^T e^T [B_v] dV_p \quad (12)$$

$$[k_{pp}] = \int_{V_p} [B_v]^T \varepsilon [B_v] dV_p \quad (13)$$

Now putting the above elemental matrices then the governing equation become

$$\partial\pi = \int_{t_1}^{t_2} \left[\{\partial \dot{q}(t)[[M_b]+[M_p]]\dot{q}(t)\}\right] - \{\partial q^T(t)[[K_b]+[K_p]]q(t)\} +$$
$$\{\partial q^T(t)[K_{pb}]v(t)\} + \{\partial v(t)[K_{bp}]q(t)\} + \{\partial v(t)[K_{pp}]v(t)\} + \left\{\sum_{i=1}^{n_f} \partial q(t)[N_w]^T Q_i(t)\right\} \quad (14)$$

Where $\delta(q)$ and $\delta(v)$ indicates the variation of the corresponding variables. Taking the integral of the above equation creates two coupled equations. The two equations shown below are coupled by the previously defined electromechanical coupling matrix k_{pb}.

$$[[m_b]+[m_p]]\ddot{q}(t) + [[k_b]+[k_p]]q(t) - [k_{pb}]v(t) = \sum_{i=1}^{n_f} [N_w]^T Q_i(t)$$
$$\text{and} \quad (15)$$
$$[k_{bp}]q(t) + [k_{pp}]v(t) = 0$$

The Eq. (15) now represents the electro-mechanical system and can be used to determine the motion of the beam. The first part of the equation defines the mechanical motion and the second part of the equation defines the electrical properties of the system. In addition to this, the system should have some type of additional mechanical damping that needs to be accounted for. If only the electrical damping is accounted for the model will over predict the actual amount of voltage generated. The amount of mechanical damping added to the model was determined from experimental results. This is done using proportional damping methods and the damping ratio that is predicted from the measured frequency response function. With the damping ratio known, proportional damping can be found as [14]

$$[C] = \alpha\{[m_b]+[m_p]\} + \beta\{[k_b]+[k_p]\} \quad (16)$$

Where α and β are determined from

$$\xi_i = \frac{\alpha}{2\omega_i} + \frac{\beta\omega_i}{2} \text{ where i} = 1,2,...n \quad (17)$$

Where ζ_i is the damping ratio found from frequency response of the structure. Hence the Eq. (15) will become

$$[[m_b]+[m_p]]\ddot{q}(t) + [[c]]\dot{q}(t) + [[k_b]+[k_p]]q(t) - [k_{pb}]v(t) = \sum_{i=1}^{n_f} [N_w]^T Q_i(t) \quad (18)$$
$$[k_{pb}]q(t) + [k_{pp}]v(t) = 0$$

From the Eq. (18) it has been seen that, due to the coupling between the mechanical and electrical components, the displacement in the piezoelectric materials induces the electric charge on the electrode. The mass matrix and stiffness matrix have been calculated by numerical integration using Gaussian quadrature. The global set of equations are found after assembling the elemental mass and stiffness matrix as

$$[M]\ddot{q}(t) + [C]\dot{q}(t) + [K]q(t) - [K_{pb}]v(t) = \sum_{i=1}^{n_f} [N_w]^T Q_i(t) \quad (19)$$
$$[K_{pb}]q(t) + [K_{pp}]v(t) = 0$$

Where [*M*], [*C*] and [*K*] are the global mass, damping and stiffness matrices of the system consisting of both beam and piezoelectric element. The terms $[K_{pb}]$ and $[K_{pp}]$ are the global coupling and dielectric matrices of the system. The above equation represents the dynamic governing equation of the Piezolaminated beam

2.3. STATE SPACE REPRESENTATION

This method is used to derive the uncoupled equations governing the motion of the free vibrations of the system in terms of principal coordinates by introducing a linear transformation between the generalized coordinates *q(t)* and the principal coordinates $\eta(t)$ [15]. The displacement vector q*(t)* can be approximated by using a transformation matrix between the generalised coordinates and the modal coordinates as

$$q(t) = \Phi\eta(t) \quad (20)$$

Where ϕ is the modal matrix containing the eigenvectors representing the vibratory modes. Representing Eq. (19) in the state-space form as

$$\begin{aligned} \{\dot{x}\} &= [A]\{X\} + [B]\{u\} \\ \{y\} &= [C]\{X\} \end{aligned} \quad (21)$$

Where [*A*] is the system matrix, [*B*] is the input matrix,[*C*] is the output matrix, {*X*} is the state vector and {*u*} is the input vector.

III. RESULT AND DISCUSSION

With consideration of the mathematical formulations discussed, a MATLAB code has been established for analysis of parabolic tapered piezolaminated beam (with different width and height taper) for output voltage and the responses so obtained has been compared with without taper beam. The developed MATLAB code has been validated and the results so obtained have been compared with the available existing results. A uniform cantilever beam of rectangular cross section is considered for validation of present code. The dimensions of the beam are (700×45×7) mm. Material properties for the beam are considered as E = 69 GPA, ρ = 2712 kg/m^3 and μ = 0.3. The free end of the beam is subjected to 1 N of impulse force. The length of beam has been divided into a number of small elements and the convergence results for different element size has been finalised. It has been found that for twenty numbers of elements it shows a good result with very less percentage of errors. The fundamental frequencies are calculated by using the present code developed and compared with the exact solution [16] presented in Table 1. From Table 1 it has been observed that results obtained from the present developed code are in good agreement with the exact results published.

Table 1 Comparison of natural frequencies of cantilever beam

Natural frequency(rad/sec)	Present code	Exact [16]	Percentage of error
ω_1	39.619	39.538	0.20
ω_2	248.846	248.569	0.11
ω_3	698.780	697.968	0.11
ω_4	1374.664	1373.338	0.09

For electro-mechanical validation the results obtained are compared with the already published results by Hwang and Park [17]and Tzou and Ye [18]. For this case a cantilever bimorph beam (100×5×1) mm has been considered which is made up of two PVDF layers. The bimorph beam has been subjected to an external voltage. Bending moment is caused due to the induced internal stresses which powers the bimorph beam to bend. The bimorph beam has been discretized into five equal finite elements. The deflections have been calculated at five nodal points by applying a unit voltage across the thickness direction. The results so obtained have been presented in Table 2. It has been found from the table that the developed code is in good agreement with the available existing results. Further it has been found that the results show a very less difference with less percentage of error.

Table 2 Transverse deflection of piezoelectric bimorph actuator

Distance(mm)from fixed end	Deflection(μm) Hwang and Park [17]	Deflection(μm) Tzou and Ye [18]	Deflection(μm) present code
20	0.0131	0.0138	0.0139
40	0.0545	0.0552	0.0554
60	0.1200	0.1240	0.1247
80	0.2180	0.2210	0.2218
100	0.3400	0.3450	0.3465

As the developed code has been validated with the existing results, further analysis has been carried out with the developed code for the same number of elements and same mass and stiffness matrices. In order to find out the frequency response of the proposed parabolic tapered beam with the application of impulse load some geometric dimensions of the beam has been considered. For these three sets of taper values of the proposed beam has been considered as 0.3, 0.5 and 0.7. The variation of both width and height tapers has been limited within this ranges. Four sets of variation has been formulated such as r_b=0.3, r_h=0.5; r_b=0.3, r_h=0.7; r_b=0.5, r_h=0.3 and r_b=0.7, r_h=0.3. in order to compare the responses with the Piezolaminated beam without taper. The various properties of the piezo patch are thickness of the piezo patch=0.5mm; Density=7500Kg/m^3; Young's Modulus=60.6 Gpa; Piezoelectric stress coefficient (e31) =16.6 C/m^2; Permittivity (ε_{33}) =25.55nF/m. The frequency response has been found by applying a load of 1 N at the free end of the proposed Piezolaminated beam. The variation of driving frequency has been from 0 to 500 Rad/Sec.

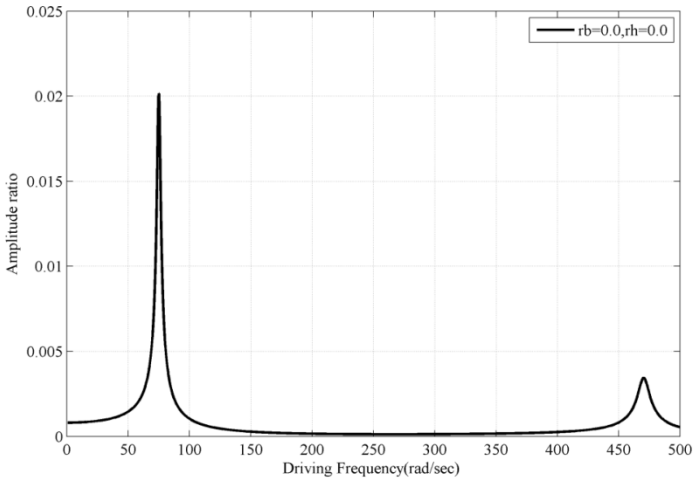

Figure 3 Frequency responses of Piezolaminated without tapered (r_b=0.0, r_h=0.0) beam.

Figure 4 represents the frequency response of Piezolaminated beam without taper (i.e. r_b=0.0, r_h=0.0). From the figure it has been found that the first and second resonant frequencies have been found at 65 rad/ sec and 475 rad/ sec where there is sudden change in amplitude caused due to resonance. The peak amplitude ratio completely depends on the amount of material damping considered in the analysis which again depends on the mass and stiffness matrices.

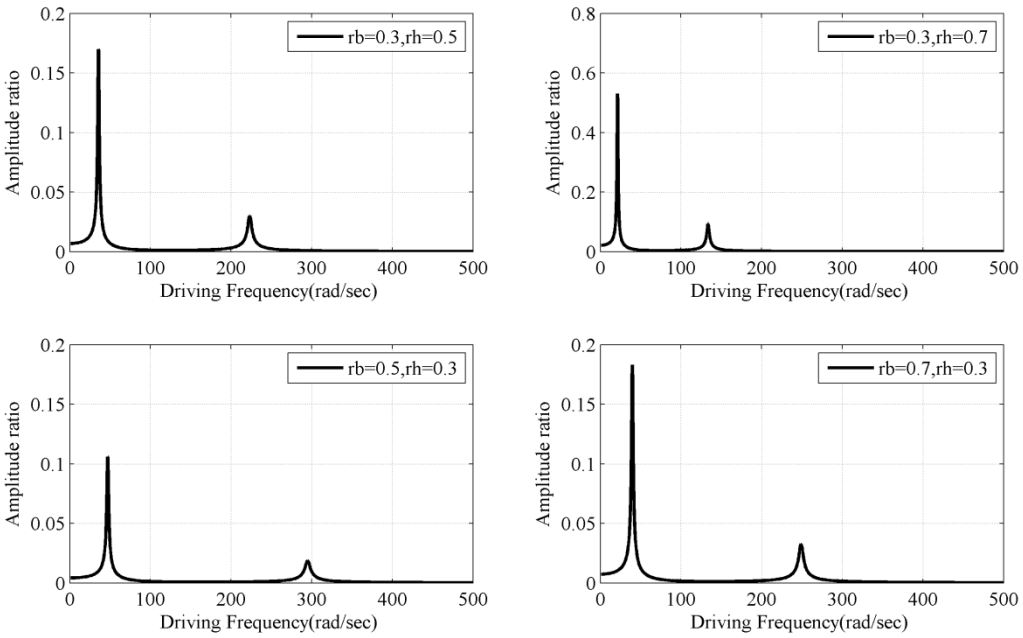

Figure 4 Frequency responses of Piezolaminated tapered (r_b=0.3, r_h=0.5; r_b=0.3, r_h=0.7; r_b=0.5, r_h=0.3 and r_b=0.7, r_h=0.3) beams

Figure 4 represents the frequency responses of the parabolic tapered beam with four sets of variation of both width and height taper such as r_b=0.3, r_h=0.5; r_b=0.3, r_h=0.7; r_b=0.5, r_h=0.3 and r_b=0.7, r_h=0.3. From the figure it has been found that by keeping the width taper fixed as 0.3, with increase in height taper from 0.5 to 0.7 the both resonant frequencies have been reduced along with the increase in amplitude ratio. The amplitude ratio has become 0.17 for r_b=0.3, r_h=0.5, where as its value coming to be 0.55 for r_b=0.3, r_h=0.7. Similarly by keeping the height taper fixed as 0.3, with increase in width taper from 0.5 to 0.7 the both resonant frequencies have been reduced along with the increase in amplitude ratio. The amplitude ratio has become 0.12 for r_b=0.5, r_h=0.3, where as its value coming to be 0.17 for r_b=0.7, r_h=0.3. From this it has been found that with increase in height taper by keeping width taper remains constant, produces an increase in amplitude ratio as compared to increase in width taper by keeping height taper remains constant.

Figure 5 represents the open circuit voltage response of a Piezolaminated beam without any taper. From the figure it has been observed that the open-circuit voltage at first resonant frequency is 2.4V/mm where as for second resonant frequency is 0.6V/mm. It has been observed that the open circuit voltage decreases at the resonant frequencies as the driving frequency increases.

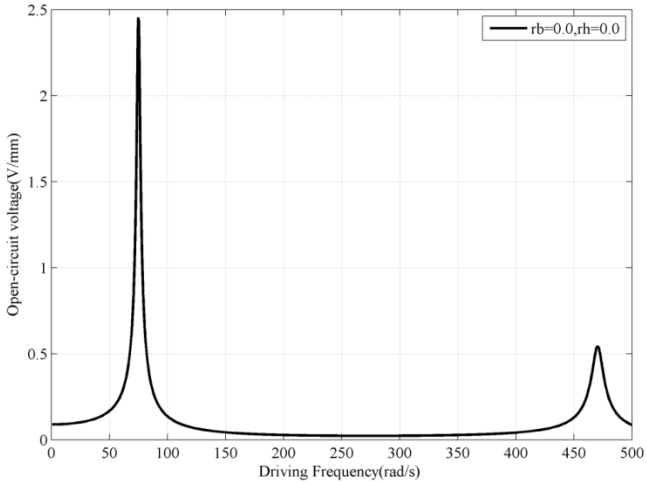

Figure 5 Voltage responses of Piezolaminated without tapered (r_b=0.0, r_h=0.0) beams

In order to find out the open circuit voltage of the proposed beam, a load of 1N has been applied at the free end. Figure 6 represents the open circuit voltage response of a Piezolaminated parabolic tapered beam with four sets of variation of both width and height taper such as r_b=0.3, r_h=0.5; r_b=0.3, r_h=0.7; r_b=0.5, r_h=0.3 and r_b=0.7, r_h=0.3.

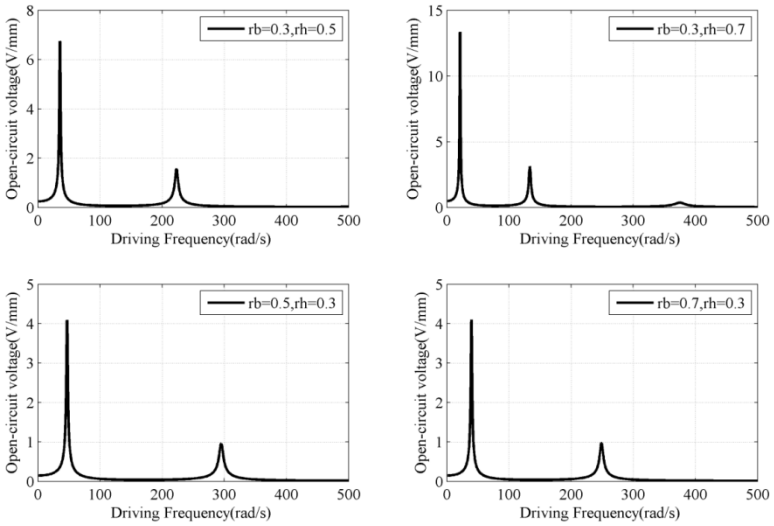

Figure 6 Voltage responses of Piezolaminated tapered (r_b=0.3, r_h=0.5; r_b=0.3, r_h=0.7; r_b=0.5, r_h=0.3 and r_b=0.7, r_h=0.3) beams

From the figure it has been found that by keeping the width taper fixed as 0.3, with increase in height taper from 0.5 to 0.7 the open circuit voltage increases to around 46% at first resonant frequency. Further by keeping the height taper remains constant as the width taper increases from 0.5 to 0.7, there has no substantial changes in open circuit voltage at the first resonant frequency. The open circuit voltage for this case is 4V/mm. The open circuit voltage response of the piezolaminated beam without taper in time domain has been shown in Figure 7. The analysis is carried out for time period of 2 sec. From the figure it has been observed that the open circuit voltage response dies out after sometime. This is due to the presence of structural damping. The damping effect due to the pressence of electric circuit is caused by principle of conservation of energy,which is responsible for reduction in amplitude. The impulse dies out faster due to this damping effect until a critical value is reached. The maximum open circuit voltage without tapered beam has been found to be 0.0093V/mm.

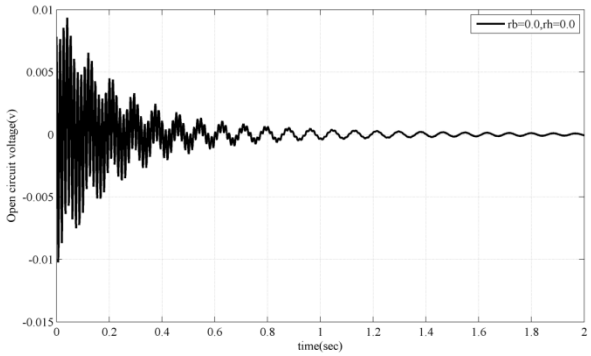

Figure 7. Time domain response of voltage generated from the Piezolaminated without taper (r_b=0.0, r_h=0.0) beam.

Figure 8 represents the time domain response of open circuit voltage of proposed Piezolaminated parabolic tapered beam with four sets of variation of both width and height taper such as r_b=0.3, r_h=0.5; r_b=0.3, r_h=0.7; r_b=0.5, r_h=0.3 and r_b=0.7, r_h=0.3.

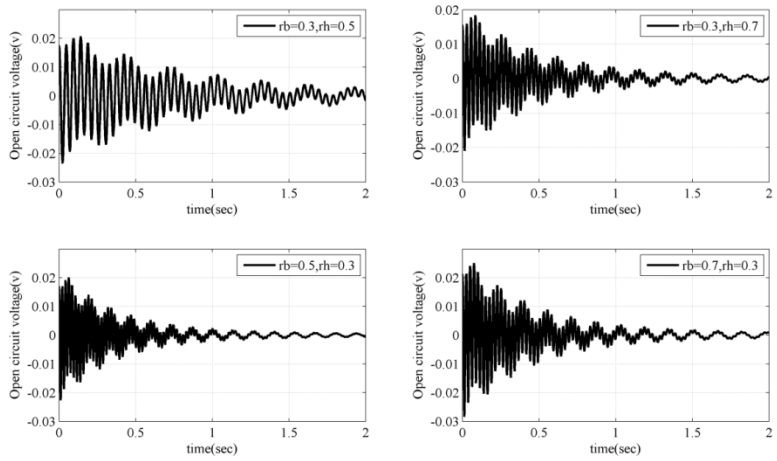

Figure 8 Time domain response of voltage generated from the Piezolaminated tapered (r_b=0.3, r_h=0.5; r_b=0.3, r_h=0.7; r_b=0.5, r_h=0.3 and r_b=0.7, r_h=0.3) beams

From the figure it has been observed that with increase in height taper from 0.5 to 0.7 by keeping the width taper remains constant, the open circuit voltage incresess from 0.0184 V/mm to 0.0206 V/mm. Similarly with increase in width taper from 0.5 to 0.7 by keeping the height taper remains constant, the open circuit voltage increases from 0.0201 V/mm to 0.0251 V/mm. From the analysis it has been observed that with increase in width taper predominates over increase in height taper for voltage generation. It has also been observed that the amplitudes of open circuit voltage decreases as the time period of vibration increases.

IV. CONCLUSION

The present article focused on voltage generation from a piezolaminated parabolic tapered beam with finite element (FE) based modelling. The beam has been modelled using the Euler-Bernoulli beam theory formulation. Two noded beam elements with two degrees of freedom at each node have been considered in order to solve the governing equation of motion. From the analysis it is observed that piezolaminated parabolic tapered beam produces more voltage for a given length of PZT patch as compared to piezolaminated beam without taper due to uniformity distribution of strain. Further it is observed that the variation of width taper keeping height taper constant, more voltage can be generated than variation of height taper keeping width taper constant.

REFERENCES

[1] S. K. Ha and Y. H. Kim, “ANALYSIS OF A PIEZOELECTRIC MULTIMORPH IN EXTENSIONAL AND FLEXURAL MOTIONS,” *J. Sound Vib.*, vol. 253, no. 5, pp. 1001–1014, Jun. 2002, doi: 10.1006/jsvi.2001.4040.

[2] “Piezoelectric Energy Harvesting with a Clamped Circular Plate: Analysis - Sunghwan Kim, William W. Clark, Qing-Ming Wang, 2005.” https://journals.sagepub.com/doi/abs/10.1177/1045389X05054044.

[3] H. A. Sodano, G. Park, and D. J. Inman, “Estimation of Electric Charge Output for Piezoelectric Energy Harvesting,” *Strain*, vol. 40, no. 2, pp. 49–58, 2004, doi: 10.1111/j.1475-1305.2004.00120.x.

[4] S. Roundy, P. K. Wright, and J. Rabaey, “A study of low level vibrations as a power source for wireless sensor nodes,” *Comput. Commun.*, vol. 26, no. 11, pp. 1131–1144, Jul. 2003, doi: 10.1016/S0140-3664(02)00248-7.

[5] S. Kapuria, “An efficient coupled theory for multilayered beams with embedded piezoelectric sensory and active layers,” *Int. J. Solids Struct.*, vol. 38, no. 50, pp. 9179–9199, Dec. 2001, doi: 10.1016/S0020-7683(01)00112-3.

[6] “Smart materials and structures—a finite element approach—an addendum: a bibliography (1997–2002) - IOPscience.” https://iopscience.iop.org/article/10.1088/0965-0393/11/5/302/meta.

[7] “Design method for piezoelectric bending generators in energy harvesting systems.” https://www.spiedigitallibrary.org/conference-proceedings-of-spie/6525/652504/Design-method-for-piezoelectric-bending-generators-in-energy-harvesting-systems/10.1117/12.715788.short?SSO=1.

[8] M. Zhu, E. Worthington, and A. Tiwari, “Design study of piezoelectric energy-harvesting devices for generation of higher electrical power using a coupled piezoelectric-circuit finite element method,” *IEEE Trans. Ultrason. Ferroelectr. Freq. Control*, vol. 57, no. 2, pp. 427–437, Feb. 2010, doi: 10.1109/TUFFC.2010.1423.

[9] “A geometric parameter study of piezoelectric coverage on a rectangular cantilever energy harvester - IOPscience.” https://iopscience.iop.org/article/10.1088/0964-1726/20/8/085004/meta.

[10] “On Nonlinear Vibration of Nonuniform Beam with Rectangular Cross-Section and Parabolic Thickness Variation | SpringerLink.” https://link.springer.com/chapter/10.1007/978-94-011-4229-8_12.

[11] D. I. Caruntu, “Classical Jacobi polynomials, closed-form solutions for transverse vibrations,” *J. Sound Vib.*, vol. 306, no. 3, pp. 467–494, Oct. 2007, doi: 10.1016/j.jsv.2007.05.046.

[12] O. Civalek and B. Ozturk, “Free vibration analysis of tapered beam-column with pinned ends embedded in Winkler-Pasternak elastic foundation,” *Geomech. Eng.*, vol. 2, no. 1, pp. 45–56, 2010, doi: 10.12989/gae.2010.2.1.045.

[13] R. Zemčík and P. Sadílek, “Modal analysis of beam with piezoelectric sensors a actuators,” 2007, Accessed: Jun. 17, 2022. [Online]. Available: http://dspace5.zcu.cz/handle/11025/1787

[14] A. R. Biswal, T. Roy, and R. K. Behera, “Optimal vibration energy harvesting from nonprismatic piezolaminated beam,” *Smart Struct. Syst.*, vol. 19, no. 4, pp. 403–413, 2017.

[15] J.-C. Trigeassou and N. Maamri, "State space modeling of fractional differential equations and the initial condition problem," in *2009 6th International Multi-Conference on Systems, Signals and Devices*, Mar. 2009, pp. 1–7. doi: 10.1109/SSD.2009.4956721.
[16] R. V. Dukkipati and J. Srinivas, *Textbook of mechanical vibrations*. 2012.
[17] "Finite element modeling of piezoelectric sensors and actuators | AIAA Journal." https://arc.aiaa.org/doi/abs/10.2514/3.11707 (accessed Jun. 17, 2022).
[18] "Analysis of piezoelastic structures with laminated piezoelectric triangle shell elements | AIAA Journal." https://arc.aiaa.org/doi/abs/10.2514/3.12907 (accessed Jun. 17, 2022).